CHEMISTRY
A EUROPEAN JOURNAL

DOI: 10.1002/chem.200801093

Natural Gum Reduced/Stabilized Gold Nanoparticles for Drug Delivery Formulations

Sheetal Dhar,[a, c] E. Maheswara Reddy,[b] Anjali Shiras,*[b] Varsha Pokharkar,*[c] and B. L. V. Prasad*[a]

Abstract: "Gellan Gum", widely used in food and confectionary industry as a thickening and gelling agent, has been employed as a reducing and stabilizing agent for the synthesis of gold nanoparticles. These nanoparticles display greater stability to electrolyte addition and pH changes relative to the traditional citrate and borohydride reduced nanoparticles. Subsequently these have been used to load anthracycline ring antibiotic doxorubicin hydrochloride. The drug loaded on these nanoparticles showed enhanced cytotoxic effects on human glioma cell lines LN-18 and LN-229.

Keywords: apoptosis · cytotoxicity · drug delivery · gold · nanostructures · natural gums

Introduction

In the present scenario, nanometer-size materials are expected to have a revolutionary impact on biology[1] and medicine.[2] Polymeric nanoparticles, dendrimers, liposomes, and metal nanoparticles are being widely explored[3] especially for drug delivery, bioimaging and biosensing.[4] Among these, metallic nanoparticles, especially gold nanoparticles (AuNPs), have attracted significant attention and are objects of great interest. Due to their unique shape, size, and surface-dependent properties, AuNPs have been exploited for their potential application in hyperthermia of cancer cells and in several other applications.[5] In clinical applications, AuNPs may have advantages over other metallic particles in terms of biocompatibility and non-cytotoxicity,[6] and can be readily conjugated to a large range of biomolecules, such as amino acids,[7] proteins/enzymes,[8] DNA,[9] and other molecular species without altering the biological activity of the conjugated species. More importantly, their facile bioconjugation and biomodification[10] has opened the door to wide biomedical applications encompassing colorimetric assays,[11] cell imaging,[12] immunostaining,[13] biosensing,[14] and DNA/drug delivery.[15] For example, antibody-modified AuNPs displayed a million-fold higher sensitivity than conventional ELISA-based assay in the detection of prostate specific antigen.[16] Perhaps, the most emerging application of AuNPs is for drug delivery. Recent reports in this category include insulin delivery by a nasal route,[17] enhanced antimicrobial activity against *E. coli* strains,[18] and ciprofloxacin-protected nanoparticles showing the ability to release the drug molecule over an extended period of time.[19]

Even though numerous synthesis methods have been employed[20] to fabricate AuNPs, lack of sufficient stability in water under strong electrolyte conditions and pH changes has impeded the applications of AuNPs. Thus, there is a need to explore various substances for the synthesis of non-toxic, biocompatible AuNPs that can control particle size, prevent aggregation, and introduce functionality to the particle surface for the conjugation of biomolecules; the search is on to look for a one-step solution to all these.[21] In this context, we have initiated our explorations to synthesize and stabilize AuNPs by using gellan gum (Kelcogel®).[22] Gellan gum (GG) is a linear, anionic heteropolysaccharide secreted

[a] S. Dhar, Dr. B. L. V. Prasad
Materials Chemistry Division
National Chemical Laboratory, Pune-411 008 (India)
Fax: (+91) 20-2590-2636
E-mail: pl.bhagavatula@ncl.res.in

[b] E. M. Reddy, Dr. A. Shiras
National Centre for Cell Sciences
Pune-411 007 (India)
Fax: (+91) 20-25692259
E-mail: anjalishiras@nccs.res.in

[c] S. Dhar, Dr. V. Pokharkar
Poona College of Pharmacy
Bharati Vidyapeeth University, Pune-411 038 (India)
Fax: (+91) 20-25439383
E-mail: varshapokharkar@rediffmail.com

Supporting information for this article is available on the WWW under http://dx.doi.org/10.1002/chem.200801093.

by the microbe *Sphingomonas elodea* (formerly known as *Pseudomonas elodea*). GG is water soluble and is commercially available as a free-flowing off-white powder. It is approved for food, non-food, cosmetic, and pharmaceutical use in the United States, Canada, Australia, and many other countries in Latin America, South America, Asia, and the European Union. According to the FDA, GG may be safely used as a direct food additive for human consumption as per 21 CFR 172.665 and appears as E418 in the European Community Directive. GG is a widely accepted ingredient within the food and pharmaceutical industry and is used in many of food products. Its water solubility, thickening, gelling, and stabilizing agent properties are some of the reason for its wide application in food and pharmaceutical industry; it is currently used in bakery fillings, confections, dairy products, and so forth. GG is also used as an ingredient in personal and oral care applications like hair-care products, creams, sunscreens, and so forth. In addition to its non-toxic properties and wide acceptance within the human food chain, GG has unique structural features that attracted our attention. Its structure consists of four linked monosaccharides (i.e., simple sugars), including one molecule of rhamnose (a sugar found in various plants), one molecule of glucuronic acid (an oxidized glucose molecule), and two molecules of glucose (a component of sucrose, which is common sugar).[23] Though gums such as gum arabic[12] have been used for stabilizing colloids for a long time, the reduction of metal nanoparticles by the gums and their utility in drug delivery is largely a new and unexplored area.[24] Thus in this paper we report the synthesis of Au NPs using GG as the reducing and capping agent, unraveling the superior stability they impart on the synthesized nanoparticles under various conditions. As mentioned above GG is characterized by many carbohydrate units and thus their capping on AuNPs should make the surface carbohydrate rich. This should enable drug loading, especially for drugs that bear many hydroxyl, amine, and other functional groups capable of forming hydrogen bonds.

For this study we selected doxorubicin hydrochloride (DOX), one of the most potent and well-known anticancer drugs; it is a member of the anthracycline ring antibiotics and is widely used in various cancer therapies.[25] Despite being widely used, the drug has a very narrow therapeutic index as its clinical use is hampered by several undesirable side-effects like cardiotoxicity and myelosuppression. Moreover, as DOX is a hydrophilic molecule, restricted transport is observed through the cellular membrane leading to minimal drug internalization and its ability to overcome biological barriers, such as the blood–brain barrier, is rather negligible. Due to this fact, free DOX cannot successfully be used for the treatment of brain tumors. Thus, various approaches have been made to target DOX to tumors, improving its efficacy and safety. One of the approaches we envisaged is the use of colloidal metal nanoparticles, especially AuNPs, for the delivery of biomolecules. Colloidal AuNPs incorporating anticancer agents can overcome resistances to drug action, thus reducing the need for higher doses and therefore reducing their toxicity towards normal cells. Despite this very few studies have been reported regarding the possibility of applying AuNPs in drug-delivery applications.[26] Here the most important obstacle is the effective loading of the drug molecules on the nanoparticle surface, their stability in physiological conditions, and the drug's availability for action when needed. Here the attachment of the drug molecule through electrostatic or hydrogen bonds may be a better strategy than covalent linkages.[27] Accordingly we report here the use of GG as reducing and stabilizing agent simultaneously for the synthesis of AuNPs and subsequent DOX loading. The bare AuNPs and DOX-loaded AuNPs were characterized in term of size, zeta potential, drug-loading efficiency, and so forth. In addition, the cytotoxicity of the DOX-loaded AuNPs was evaluated by using two different well-established glioma cell lines, that is, LN-18 and LN-229, by in vitro MTT assays.[28] Gliomas are the most common primary brain tumors in adults.[29] They are highly invasive and are resistant to most conventional therapies including chemotherapy and radiation therapy. Immunofluroscence studies were conducted for further confirmation of apoptosis induced by DOX-loaded AuNPs in these cell lines.

Results and Discussion

In the present study, we took advantage of the reducing, stabilizing, and biocompatible properties of GG for the synthesis of AuNPs. It was envisaged that this strategy would also provide sufficient exposed functional moieties on AuNPs that will aid in the subsequent attachment of large number of biomolecules for drug-delivery applications (Scheme 1). The AuNPs synthesized were thoroughly characterized by a range of techniques including UV/Vis spectroscopy, powder X-ray diffraction (XRD), transmission electron microscopy

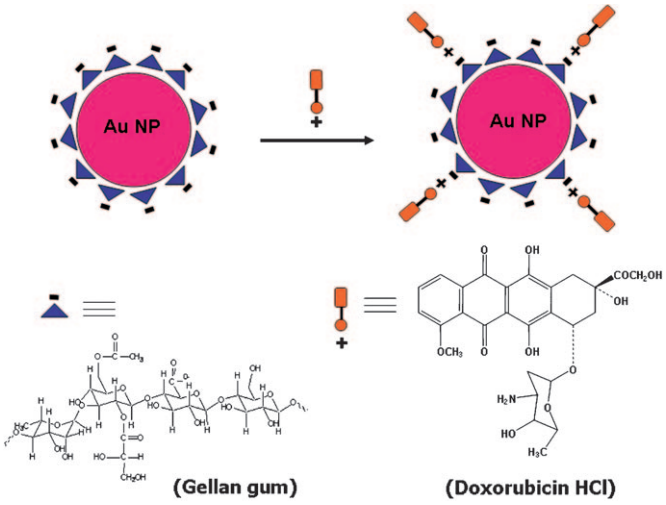

Scheme 1. Schematic diagram showing anionic gellan gum gold nanoparticles and subsequent loading of cationic doxorubicin HCl on gellan gum capped gold nanoparticles.

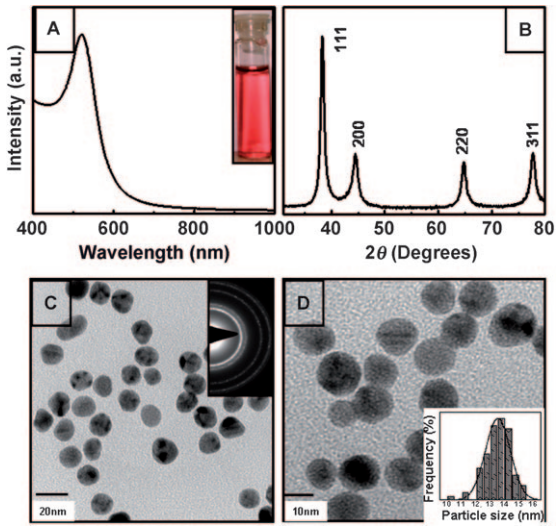

Figure 1. A) UV/Vis absorption spectra of gellan gum reduced gold nanoparticles. B) XRD patterns of the gold nanoparticles. C),D) HRTEM images recorded of blank gold nanoparticles reduced by 0.02% gellan gum. Inset C),D) shows electron diffraction pattern and particle size distribution of gold nanoparticles respectively.

(TEM), and selected area electron diffraction (SAED) as displayed in Figure 1. It is known that AuNPs exhibit surface plasmon resonance at 520 nm,[20] clearly seen in Figure 1A. The TEM images recorded from as-synthesized AuNPs (Figure 1C and D) reveal that the nanoparticles are well dispersed with a narrow size distribution and an average size of 13 ± 1 nm (inset, Figure 1D). The SAED pattern (inset Figure 1C) of the AuNPs is indexed to the 111, 200, 220, 311 Bragg reflections of face-centered cubic (fcc) gold structure; this is also confirmed from the powder X-ray diffract gram recorded from the sample (Figure 1B).

A very important stipulation for the drug delivery applications of nanoparticles is their stability over time and under different pH and electrolytic conditions.[30] The GG-reduced AuNPs were extremely stable over time and did not show any noticeable variation in either UV/Vis spectra, particle shape and size even after few months of storage at room temperature (data not shown). Significantly they showed no discernible change in the intensity or position of the absorbance at $\approx$520 nm in the pH window of 3–10 (Figure 2A). Even the addition of NaCl up to 0.1 M caused no major aggregation (Figure 2B), thus meeting the stipulations laid out for the utility of these particles for drug-delivery applications. As the surface plasmon resonance position is very sensitive to the aggregation, the minimal change in its position under the above experimental conditions indicates the extra stability of GG-capped AuNPs. In comparison other AuNPs systems obtained by borohydride or citrate reduction routes aggregate at the slightest change in their pH and electrolyte environments.[30]

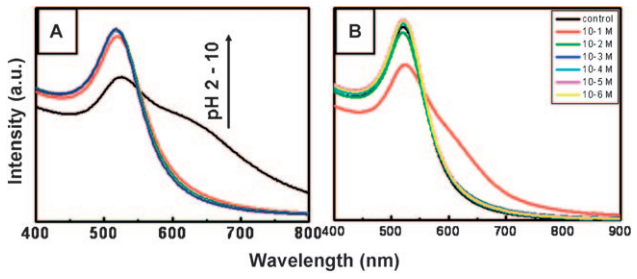

Figure 2. The pH (A) and salt (B) studies of gellan gum reduced gold nanoparticles.

Having established the formation of stable nanoparticles, we subsequently proceeded to investigate the drug loading. Based on the UV/Vis absorbance studies (see Experimental Section for details), the loading efficiency of DOX on GG-reduced nanoparticles was determined to be 75%. At neutral pH the zeta potential of GG ($pK_a=3.1$)-reduced AuNPs was -38.25 mV. This clearly indicated that the AuNPs were wrapped with the anionic GG, which helps nanoparticles to attain stability by electrostatic means. The zeta potential of DOX (pKa = 8.2) loaded AuNPs was -30.00 mV. The slight decrease in the zeta potential is ascribed to the presence of positively charged DOX. The small decrease in the charge even at 75% loading of DOX indicates that other attractive forces including hydrogen bonding could be playing a major role facilitating the drug-loading process. It is clear that even after DOX loading, the AuNPs remain in suspension by their electrostatic repulsion and maintain the negative charge on the surface. We studied the pH dependent stability of DOX-loaded nanoparticles (Figure 3A). It was observed that these AuNPs were very stable between pH 4.0 to 8.0. Below pH 4.0 and above 8.0, the addition of DOX solution to the colloidal AuNPs caused the particles to aggregate. The retention of absorbance intensity corresponding to

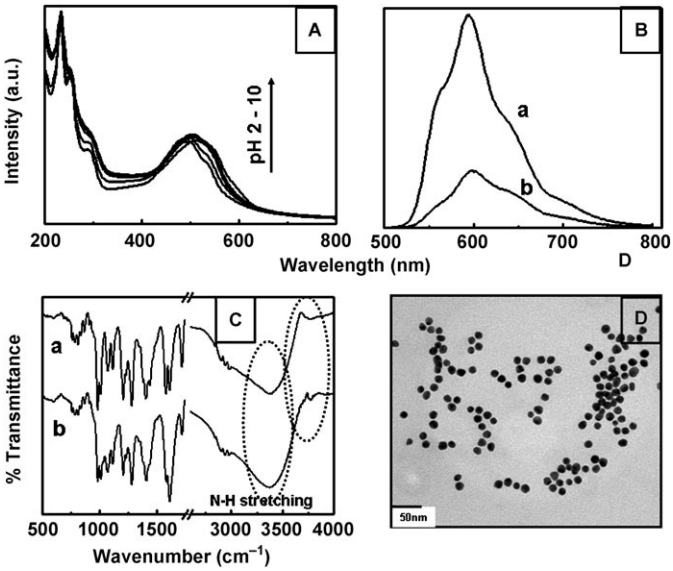

Figure 3. A) pH study of DOX-loaded gold nanoparticles. B) Fluorescence spectra of a) DOX solution and b) DOX-loaded gold nanoparticles. C) FTIR spectra of a) DOX solution and b) DOX-loaded gold nanoparticles. D) HRTEM image of redispersed DOX-loaded gold nanoparticles.

DOX also shows that the drug is stable in this pH window. The stability of DOX molecule after loading on AuNPs was studied by using fluorescence spectroscopy. The emission spectra of DOX in solution and DOX-loaded AuNPs were recorded from 490 to 800 nm at a fixed excitation of 480 nm; the spectra recorded are shown in Figure 3B. There was no major change in the spectral profile in DOX-loaded AuNPs, and the peaks at 597 and 635 nm, which are observed for pure DOX, were retained. The decrease in peak intensities after interaction with GG-reduced AuNPs can be explained by slight quenching of DOX emission that is known occur when fluorophores are close to metal nanoparticle surface.[31] However, the preservation of the fluorescence signature supports the claim that DOX structure is retained following complexation with nanoparticles;[32] this fact is very important for its biological activity. The hydrogen-bonding hypothesis between protonated amine group of the DOX molecule with GG on the surface AuNPs is also supported by FTIR; N–H stretching of the pure DOX at 3777 cm^{-1} is shifted to 3374 cm^{-1} in case of DOX-loaded AuNPs (Figure 3C). The TEM images of DOX-loaded AuNPs also retain their morphology, giving credence to the assertion that DOX loading neither cause much change in their size nor lead to any aggregation (Figure 3D).

To explore the potential of AuNPs as drug delivery carriers, we first determined the cytotoxic effect of GG-reduced AuNPs as well as the sensitivity of DOX-loaded AuNPs on human glioma cell lines. The in vitro cytotoxicity of different formulations, namely, free DOX, DOX-loaded AuNPs, control AuNPs with no drug, and only culture media for negative control, was investigated in human glioma cell lines (LN-18 and LN-229) by using an MTT assay. The results after 24 and 48 h are shown in Figures 4 and 5.

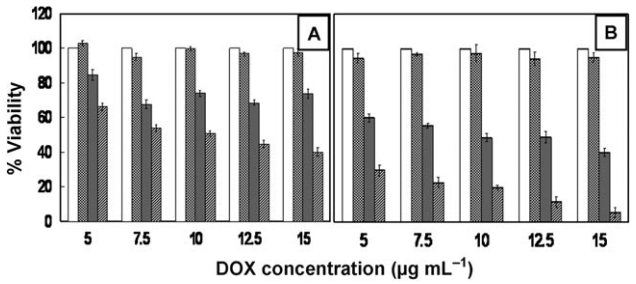

Figure 4. Viability of LN-18 after 24 (A) and 48 h (B), after exposure to (from left to right): control (media), blank nanoparticles, DOX solution, and DOX-loaded gold nanoparticles.

The wells that received only media were regarded as a negative control with a cell viability of 100%. No cytotoxicity effect of GG-reduced AuNPs was observed on either cell lines as the cell viability did not decrease, even after 72 h of experiment. It showed that the AuNPs were well tolerated by both cell lines and had no effect on cell viability, which further confirmed the biocompatibility of the AuNPs.[6] Figure 4A and B show the percent viability of LN-18 cell line

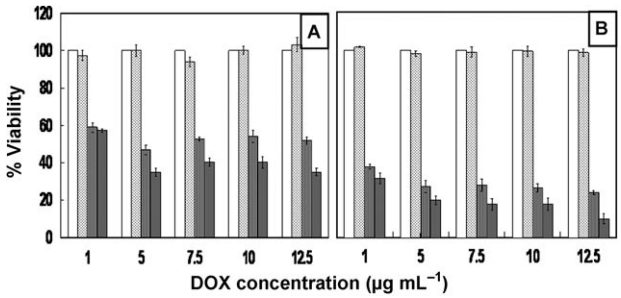

Figure 5. Viability of LN-229 after 24 (A) and 48 h (B) after exposure to (from left to right): control (media), blank nanoparticles, DOX solution, DOX-loaded gold nanoparticles.

after exposure to DOX, in pure solution form and as loaded on nanoparticles for 24 and 48 h, respectively. It is to be noted that at each concentration the drug-loaded Au NPs were taken such that the DOX concentration was similar to that in free solution, making a direct comparison possible. At the end of 24 h, the pure DOX solution had not caused any significant inhibition of the cell growth, whereas DOX-loaded AuNPs exhibited strongly enhanced cytotoxicity, with values ranging from about 50% at 7.5 μg mL^{-1} to 40% at 15.0 μg mL^{-1}. After 48 h of incubation, all the LN-18 cells cultured in the presence of DOX-loaded AuNPs within the checked concentration range (5.0–15.0 μg mL^{-1}) showed more significant reduction in viability. At the highest concentration 15.0 μg mL^{-1}, the cell viability was decreased to 5% at the end of 48 h. The maximum decrease in cell viability achieved with 15.0 μg mL^{-1} free DOX solution was 40% at the end of 48 h, indicating a slower rate of decrease (50% to 40%) as compared to the DOX-loaded GG-Au NPs (40% to 5%). In case of human glioma cell line LN-229 (Figure 5), free DOX and DOX-loaded AuNPs gradually increase their cytotoxicity with increasing concentration; however, the cytotoxicity was dominated by DOX-loaded GG-Au NPs. At the end of 24 h and 48 h incubation, the decrease in cell viability with DOX-loaded nanoparticles in the concentration range studied (5.0–12.5 μg mL^{-1}) was between 57–34% and 31–10%, respectively. Many groups have studied the incorporation of DOX in colloidal carriers. The increase of DOX cytotoxicity compared to the solution has already been observed with polymeric nanoparticles, micelles, and liposomes carrying doxorubicin.[33] The AuNPs employed here also turn out to be very effective DOX carriers, comparable to the intricate systems mentioned above. In our study we observed a steep increase in the cytotoxicity in both the cell lines when AuNPs loaded with DOX were used. This indicated that DOX-loaded AuNPs are more potent than free DOX. A possible explanation for the activity enhancement of DOX-loaded AuNPs is the improved internalization of drug-loaded NPs by an endocytosis mechanism, compared to the passive diffusion mechanism of free DOX into cells.[34] Moreover, it was found that binding of doxorubicin to nanoparticles increased the efficacy against glioma tumors.[25a]

DOX is known to induce apoptosis (i.e., programmed death of tumor cells) by blocking the cell cycle and inhibiting the DNA polymerase enzyme.[35] We analyzed the apoptosis on LN-18 and LN-229 induced by DOX-loaded–GG-reduced AuNPs by using phase-contrast and confocal microscope techniques. For comparison, the morphology of the untreated cells was initially observed by phase contrast microscope. After incubation of both cell lines with DOX-loaded AuNPs, free DOX solution, and blank AuNPs (concentration same as MTT cytotoxic assay) for 24 h, the morphology of both cell lines changed significantly as compared to the untreated cells (Figure 6 and SI-1 in Supporting Information). The cells shrunk to a spherical shape and most of them were detached from the cover slip. The cytoplasm of the cell was distributed badly and formed the apoptotic bodies, and some of the cells were budding. Because of apoptosis most of the cells were detached from the cover slips and washing further removed the apoptotic cells, but the main apoptosis features like cell shrinkage, chromatin condensation, and nuclei fragmentation were clearly observed with the help of confocal microscopy. CLSM images clearly demonstrated the apoptosis-induced cell death by DOX-loaded AuNPs on human glioma cell lines LN-18 and LN-229.

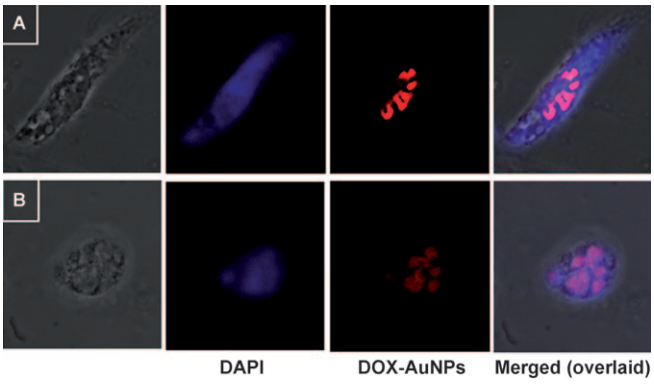

Figure 6. A) LN-18, B) LN-229. Confocal microscopy images to demonstrate the apoptosis induced by DOX-loaded gold nanoparticles. Cells were initially cultured for 24 h, followed by addition of DOX nanoparticles, then continually cultured for 24 h before examination.

In conclusion, we have reported a novel method for synthesis of gold nanoparticles by using natural, biocompatible GG and the feasibility of using AuNPs as carriers for the delivery of the cationic anthracycline drug, doxorubicin hydrochloride (DOX). We have demonstrated the successful loading of DOX onto AuNPs and their concentration-related increased cytotoxicity in human glioma cell lines. Confocal images confirmed the apoptotic-induced activity of DOX. These results are promising and warrant further investigation to reveal the in vivo cytotoxic capacity of DOX-loaded AuNPs in cancer therapy, especially brain tumor. The carbohydrate-rich nanoparticle surface may facilitate better transport of the loaded drug across blood–brain barrier. As such, this is very generic and can be expanded to include the delivery of other biologically active molecules as well. Our group has been exploring other naturally occurring gums, also as reducing and capping agents for gold nanoparticle synthesis, some of which showed very promising results greatly enhancing the attractiveness of the present study.

Experimental Section

Materials: Doxorubicin hydrochloride was a gift sample from RPG Life Sciences Limited, Mumbai (India). Hydrochloroauric acid ($HAuCl_4$) was obtained from Aldrich Chemicals. GG was a gift sample from CP Kelco, Atlanta (USA). The human glioma cell lines LN-18 and LN-229 were procured from American type culture collection (ATCC, USA). The yellow tetrazolium MTT (3-(4, 5-dimethylthiazolyl-2)-2, 5-diphenyltetrazolium bromide) was obtained from Sigma-Aldrich (USA). All the samples were prepared in a Millipore milli Q water system.

Synthesis of gold nanoparticles: In a typical experiment, an aqueous solution of $HAuCl_4$ (1×10^{-4} M, 100 μL) was reduced to gold nanoparticles (AuNPs) by heating in a an aqeuous solution of GG (100 mL) using 0.02 % w/v. After addition of $HAuCl_4$ the pH of the solution was adjusted with sodium hydroxide to between 11–12 to yield ruby-red AuNPs on boiling. The ruby-red solution yielded an absorbance maximum at 518 nm. Control experiments revealed that the optimum particle size distribution and stability were all achieved at the conditions specified above. The dependence of particle size on temperature and pH has been studied in detail and will be reported elsewhere.

UV/Vis spectroscopy measurements: The change in surface plasmon resonance of AuNPs, before and after loading of DOX, was monitored by UV/Vis/NIR spectroscopy measurements, carried out on a V-570 model Jasco Dual Beam spectrophotometer operating at a resolution of 2 nm.

Loading of doxorubicin hydrochloride onto gold nanoparticles: A calculated amount of DOX was added to a dispersion of AuNPs, obtained as described above, resulting in a final DOX concentration of 10^{-4} M in solution. The solution was then incubated for 24 h at room temperature and then centrifuged at 20000 rpm for 0.5 h. The pellets thus obtained after centrifugation were separated from the supernatant solution and redispersed in milli Q water prior for further characterization. The free DOX present in the supernatant was determined by measurements of its UV absorbance and the percentage loading of DOX on AuNPs was estimated by following formula: % loading = [(total amount of DOX added − amount of DOX in supernatant)/Total amount of DOX added] × 100.

X-ray diffraction (XRD) measurements: Films prepared on glass substrates by simple solvent evaporation of dispersions of GG-reduced AuNPs were used for X-ray diffraction measurements. The diffraction measurements was carried out on a PANalytical Xpert PRO instrument operating at 40 kV and a current of 30 mA at a scan rate of $0.38°\,min^{-1}$.

High-resolution transmission electron microscopy (HRTEM) measurement: Samples for HRTEM analysis were prepared by drop casting of GG-reduced AuNPs and DOX-loaded AuNPs solutions on carbon-coated copper grids and allowed to dry at room temperature. Measurements were done on a TECHNAI G^2 F30 S-TWIN instrument operated at an accelerated voltage of 300 kV with a lattice resolution of 0.14 nm and point image resolution of 0.20 nm. The particle size analysis was carried out using Gattan software (Pleasanton, CA, USA).

Zeta potential measurements: The surface charge of AuNPs before and after loading of DOX was determined by measurement of zeta potential, determined by using a zeta potential analyzer, Brookhaven Instruments Corporation, NY. The average zeta potential of nanoparticulate dispersion was determined as such without any dilution.

Fourier transform infrared spectroscopy (FTIR) measurements: FTIR spectra of DOX bound to the AuNPs were recorded on a Perkin–Elmer Spectrum-One instrument in the diffuse reflectance mode at a resolution of 4 cm^{-1} in the range of 400–4000 cm^{-1} in KBr pellets. For comparison, FTIR spectrum of pure DOX was also recorded.

Fluorescence spectroscopy measurements: Fluorescence spectroscopy measurements were carried out to study the stability of DOX after binding with GG-reduced AuNPs. Fluorescence spectra of free DOX solution and DOX-loaded AuNPs were recorded on Cary Eclipse Fluorescence Spectrophotometer, Varian.

In vitro cytotoxicity assay

Cell line and growth medium: Human glioma cell lines LN-18 and LN-229 were cultured in Dulbecco's modified eagle's medium (DMEM) supplemented with 1.5 gm L^{-1} sodium bicarbonate, 4 mM glutamine and 5–10% fetal bovine serum (Gibco, USA) The cultures were maintained in a humidified atmosphere of 5% CO_2 at 37 °C in an incubator.

Cell preparation: For cytotoxicity testing, the cells were utilized when they reached 60–80% confluent. The cells were diluted as needed and seeded as 4×10^3 for LN18 and 3×10^3 for LN229 in 100 μL of media per well, sequentially plated in flat bottom 96-well plates (Becton Dickinson Labwane, USA). This number of cells was selected to avoid potential over confluence of the cells by the end of the four-day experiment while still providing enough cells for adequate formazan production. After plating, the 96-well plates were then incubated for 24 h to allow adherence of the cells prior to the administration of various samples for testing.

Drug addition: The cells were incubated for 24 h at 37 °C and the details are mentioned above. The culture medium were replaced with 200 μL of solution containing fresh medium plus DOX-loaded AuNPs or free DOX solution, so that the final concentration variations of DOX-Au NPs or DOX were realized. To evaluate possible effect of blank AuNPs on cell viability, cells were also incubated with blank AuNPs. Control wells containing cells received only 200 μL of medium. After addition of all the test samples, the plates were returned to the CO_2 incubator. The study was conducted further up to a period of 72 h to allow both time-dependent and concentration-dependent drug-induced cytotoxicity. Furthermore, cells could be maintained in wells for this period without the need for refeeding. The antiproliferative effect of DOX was analyzed by use of the MTT assay[31] to assess the cytotoxicity of the DOX-loaded AuNPs in comparison with free DOX and blank AuNPs. The percentage cell viability was then determined. All experiments were performed in triplicate.

MTT assay: This assay was based on the measurement of the mitochondrial activity of viable cells by the reduction of the tetrazolium salt MTT (3-(4,5-dimethyathiazol-2-yl)-2, 5-diphenyl tetrazolium bromide) to form a blue water-insoluble product, formazan. After addition of various concentrations of free DOX and DOX-loaded AuNPs, cells were again incubated. After 24 h of incubation, MTT (5 mg mL^{-1}, 20 μL) was added to respective set of cells and the plates were incubated for an additional 4 h. After 4 h of incubation, the medium was removed and DMSO (200 μL, Sigma-Aldrich, USA) was added to dissolve the formazan crystals resulting from the reduction of the tetrazolium salt only by metabolically active cells. The absorbance of dissolved formazan was measured at 570 nm using a Bio-Rad microplate reader (Model 680). Since the absorbance directly correlated with the number of viable cells, the percent viability was calculated from the absorbance.

Confocal laser scanning microscopy (CLSM): Confocal laser scanning microscopy was used to detect the apoptotic activity and uptake of DOX on cell lines. Before addition of various formulations, LN-18 and LN-229 cells were seeded at low density in 24 well plates (Becton Dickinson Labware, USA) on cover slips (ERIE scientific company, USA) and grown for 24 h to achieve semiconfluent cultures. When the cells were attached to the surface of the cover slips as a monolayer, they were incubated with different concentrations of DOX-loaded AuNPs, free DOX solution, and blank nanoparticles. The cells were further incubated for 24 h at 37 °C and 5% CO_2 in a humidified environment. After incubation, cells on the cover slip were washed with ice-cold phosphate buffered saline (PBS, Himedia, Mumbai, India) and fixed in 4% paraformaldehyde (Sigma-Aldrich, USA) for 10 min at room temperature. After two more rinses in PBS, cells were blocked in 5% BSA (ICN biomedicals, Germany) in PBS for 30 min at room temperature. Cells were washed three times in PBS in the dark and then incubated with DAPI (Molecular probes, USA) for 10 min. Cells were mounted with mounting medium containing DABCO (Sigma-Aldrich, USA). Confocal images were acquired using Zeiss LSM 510 confocal microscope (Germany). More representative confocal microscopy images are available in Supporting Information.

Acknowledgement

The authors thank DST, New Delhi for funding to this work through the DST-Unit on Nano Science and Technology (DST-UNANST) at NCL.

[1] C. Zandonella, *Nature* **2003**, *423*, 10–12.
[2] J. L. West, N. J. Halas, *Curr. Opin. Biotechnol.* **2000**, *11*, 215–217.
[3] a) J. Kreuter, *Adv. Drug Delivery Rev.* **2001**, *47*, 65–81; b) L. E. V. Vlerken, M. M. Amiji, *Expert Opin. Drug Delivery* **2006**, *3*, 205–216; c) G. Han, P. Ghosh, V. Rotello, *Nanomedicine* **2007**, *2*, 113–123.
[4] a) S. Shukla, A. Priscilla, M. Banerjee, R. R. Bhonde, J. Ghatak, P. V. Satyam, M. Sastry, *Chem. Mater.* **2005**, *17*, 5000–5005; b) P. Alivisatos, *Nat. Biotechnol.* **2004**, *22*, 47–52; c) W. C. W. Chan, S. Nie, *Science* **1998**, *281*, 2016–2018.
[5] a) P. K. Jain, X. Huang, I. H. El-Sayed, M. A. El-Sayed, *Acc. Chem. Res.* **2008**, DOI:10.1021/ar7002804; b) X. Huang, I. H. El-Sayed, W. Qian, M. A. El-Sayed, *J. Am. Chem. Soc.* **2006**, *128*, 2115–2120.
[6] a) R. Shukla, V. Bansal, M. Chaudhary, A. Basu, R. R. Bhonde, M. Sastry, *Langmuir* **2005**, *21*, 10644–10654; b) E. E. Connor, J. Mwamuka, A. Gole, C. J. Murphy, M. D. Wyatt, *Small* **2005**, *1*, 325–327.
[7] a) P. R. Selvakannan, S. Mandal, S. Phadtare, A. Gole, R. Pasricha, S. D. Adyanthaya, Murali Sastry, *J. Colloid Interface Sci.* **2004**, *269*, 97–102; b) P. R. Selvakannan, S. Mandal, S. Phadtare, R. Pasricha, M. Sastry, *Langmuir* **2003**, *19*, 3545–3549.
[8] a) C. M. Niemeyer, B. Ceyhan, *Angew. Chem.* **2001**, *113*, 3798–3801; *Angew. Chem. Int. Ed.* **2001**, *40*, 3685–3688; b) A. Gole, C. Dash, V. Ramakrishnan, S. R. Sainkar, A. B. Mandale, M. Rao, Murali Sastry, *Langmuir* **2001**, *17*, 1674–1679; c) A. Gole, C. Dash, C. Soman, S. R. Sainkar, M. Rao, M. Sastry, *Bioconjugate Chem.* **2001**, *12*, 684–690.
[9] a) A. P. Alivisatos, X. Peng, T. E. Wilson, C. L. Loweth, M. P. Bruchez Jr, P. G. Schultz, *Nature* **1996**, *382*, 609–611; b) A. Kumar, M. Pattarkine, M. Bhadbhade, A. B. Mandale, K. N. Ganesh, S. S. Datar, C. V. Dharmadhikari, M. Sastry, *Adv. Mater.* **2001**, *13*, 341–344.
[10] E. Katz, I. Willner, *Angew. Chem.* **2004**, *116*, 6166–6235; *Angew. Chem. Int. Ed.* **2004**, *43*, 6042–6108.
[11] C. D. Medley, J. E. Smith, Z. Tang, Y. Wu, S. Bamrungsap, W. Tan, *Anal. Chem.* **2008**, *80*, 1067–1072.
[12] V. Kattumuri, K. Katti, S. Bhaskaran, E. J. Boote, S. W. Casteel, G. M. Fent, D. J. Robertson, M. Chandrasekhar, R. Kannan, K. V. Katti, *Small* **2007**, *3*, 333–341.
[13] J. Roth, *Histochem. Cell Biol.* **1996**, *106*, 79–92.
[14] L. Olofsson, T. Rindzevicius, I. Pfeiffer, M. Kall, F. Hook, *Langmuir* **2003**, *19*, 10414–10419.
[15] C. M. Niemeyer, *Angew. Chem.* **2001**, *113*, 4254–4287; *Angew. Chem. Int. Ed.* **2001**, *40*, 4128–4158.
[16] J. M. Nam, C. S. Thaxton, C. A. Mirkin, *Science* **2003**, *301*, 1884–1886.
[17] H. M. Joshi, D. R. Bhumkar, K. Joshi, V. Pokharkar, M. Sastry, *Langmuir* **2006**, *22*, 300–305.
[18] H. Gu, P. L. Ho, E. Tong, L. Wang, B. Xu, *Nano Lett.* **2003**, *3*, 1261–1263.
[19] R. T. Tom, V. Suryanarayanan, P. G. Reddy, S. Baskaran, T. Pradeep, *Langmuir* **2004**, *20*, 1909–1914.
[20] a) M. C. Daniel, D. Astruc, *Chem. Rev.* **2004**, *104*, 293–346; b) M. Brust, M. Walker, D. Bethell, D. J. Schiffrin, R. Whyman, *J. Chem. Soc. Chem. Commun.* **1994**, *7*, 801–802.
[21] K. Tsuchida, T. Murakami, *Mini-Rev. Med. Chem.* **2008**, *8*, 175–183.
[22] Kelcogel® for details see http://www.cpkelco.com/food/gellan.html.

[23] a) M. O'Neill, R. Selvendran, A. J. Morris, *Carbohydr. Res.* **1983**, *124*, 123–133; b) P. E. Jansson, B. Lindberg, P. A. Sandford, *Carbohydr. Res.* **1982**, *124*, 135–139.
[24] Y. M. Mohan, K. M. Raju, K. Sambasivudu, S. Singh, B. Sreedhar, *J. Appl. Polym. Sci.* **2007**, *106*, 3375–3381.
[25] a) S. C. J. Steiniger, J. Kreuter, A. S. Khalansky, I. N. Skdan, A. I. Bobruskin, Z. S. Smirnova, S. E. Severin, R. Uhl, M. Kock, K. D. Geiger S. E. Gelperina, *Int. J. Cancer* **2004**, *109*, 759–767; b) S. Mitra, U. Gaura, P. C. Ghosha, A. N. Maitra, *J. Controlled Release* **2001**, *74*, 317–323.
[26] a) R. K. Visaria, R. J. Griffin, B. W. Williams, E. S. Ebbini, G. F. Paciotti, C. W. Song, J. C. Bischof, *Mol. Cancer Ther.* **2006**, *5*, 1014–1020; b) G. F. Paciotti, L. Myer, D. Weinreich, D. Goia, N. Pavel, R. E. McLaughlin, L. Tamarkin, *Drug Delivery* **2004**, *11*, 169–183.
[27] J. D. Gibson, B. P. Khanal, E. R. Zubarev, *J. Am. Chem. Soc.* **2007**, *129*, 11653–11661.
[28] T. Mosmann, *J. Immunol. Methods* **1983**, *65*, 55–63.
[29] a) A. Kleihues, P. H. Ohgaki, *Toxicol. Pathol.* **2000**, *28*, 164–170; b) P. Kleihues, D. N. Louis, B. W. Scheithauer, l. B. Rorke, G. Reifenberger, P. C. Burger, W. K. Cavenee, *J. Neuropathol. Exp. Neurol.* **2002**, *61*, 215–225.
[30] L. L. Rouhana, J. A. Jaber, J. B. Schlenoff, *Langmuir* **2007**, *23*, 12799–12801.
[31] C. Fan, S. Wang, J. W. Hong, G. C. Bazan, K. W. Plaxco, A. J. Heeger, *Proc. Natl. Acad. Sci. USA* **2003**, *100*, 6297–6301.
[32] a) K. K. Karukstis, E. H. Z. Thompson, J. A. Whiles, R. J. Rosenfeld, *Biophys. Chem.* **1998**, *73*, 249–263; b) K. A. Janes, M. P. Fresneau, A. Marazuela, A. Fabra, M. J. Alonsoa, *J. Controlled Release* **2001**, *73*, 255–267.
[33] S. Bennis, C. Chapey, P. Couvreur, J. Robert, *Eur. J. Cancer* **1994**, *30*, 89–93.
[34] H. S. Yoo, K. H. Lee, J. E. Oh, T. G. Park, *J. Controlled Release* **2000**, *68*, 419–431.
[35] A. Skladanowski, J. Konopa, *Biochem. Pharmacol.* **1993**, *46*, 375–382.

Received: June 5, 2008
Published online: October 10, 2008

